

A peptidoglycan monomer with the glutamine to serine change and basic peptides bind in silico to TLR-2 (403–455)

Yufeng Li · Clay L. Efferson ·
Rajagopal Ramesh · George E. Peoples ·
Patrick Hwu · Constantin G. Ioannides

Received: 16 May 2010/Accepted: 8 December 2010/Published online: 28 December 2010
© Springer-Verlag 2010

Abstract Bacterial cell wall polysaccharides, such as PGN, bind and activate TLR-2, NOD2 and PGRP on monocytes/macrophages and activate inflammation. We found that the peptides containing basic amino acids (cations) at *N*-terminus and tyrosine at *C*-terminus interfered with activating ability of PGN. This finding is significant because the ECD of TLR-2 *in vivo* encounters a large number of proteins or peptides. Some should bind ECD and “pre-form” TLR-2 to respond or not to its activators, although they cannot activate TLR-2 alone. TLR-2 is receptor for a large number of ligands, including lipopeptides and bacterial cell wall glycoproteins. A binding site for lipopeptides has been identified; however, a binding site for soluble or multimeric PGN has not been proposed. To identify the candidate binding sites of peptides and PGN on TLR-2, we modeled docking of peptides and of the PGN monomer (PGN-S-monomer) to extracellular domain

(ECD-TLR-2) of the unbound TLR-2. Quantification, *in silico*, of free energy of binding (DG) identified 2 close sites for peptides and PGN. The PGN-S-monomer binding site is between amino acids TLR-2, 404–430 or more closely TLR-2, 417–428. The peptide-binding site is between amino acids TLR-2, 434–455. Molecular models show PGN-S-monomer inserts its *N*-acetyl-glucosamine (NAG) deep in the TLR-2 coil, while its terminal lysine interacts with inside (Glu⁴⁰³) and outside pocket (Tyr³⁷⁸). Peptides insert their two *N*-terminal arginines or their *C*-terminal tyrosines in the TLR-2 coil. PGN did not bind the lipopeptide-binding site in the TLR-2. It can bind the *C*-terminus, 572–586 (DG = 0.026 kcal), of “lipopeptide-bound” TLR-2. An additional, low-affinity PGN-binding site is TLR-2 (227–237). MTP, MDP, and lysine-less PGN bind to TLR-2, 87–113. This is the first report identifying candidate binding sites of monomer PGN and peptides on

Electronic supplementary material The online version of this article (doi:[10.1007/s00262-010-0959-1](https://doi.org/10.1007/s00262-010-0959-1)) contains supplementary material, which is available to authorized users.

Y. Li (✉) · P. Hwu
Departments of Melanoma Medical Oncology,
The University of Texas MD Anderson Cancer Center,
1515 Holcombe Blvd, Houston, TX 77030, USA
e-mail: yim_lee80@hotmail.com

C. L. Efferson
Departments of Gynecologic Oncology, The University of Texas
MD Anderson Cancer Center, 1515 Holcombe Blvd,
Houston, TX 77030, USA

R. Ramesh
Departments of Thoracic Surgery, The University of Texas MD
Anderson Cancer Center, 1515 Holcombe Blvd,
Houston, TX 77030, USA

G. E. Peoples
Department of Surgery, General Surgery Service,
Brooke Army Medical Center, 3851 Roger Brooke Drive,
Fort Sam, Houston, TX 78234, USA

Y. Li · C. G. Ioannides (✉)
Departments of Experimental Therapeutics,
The University of Texas MD Anderson Cancer Center,
1515 Holcombe Blvd, P.O. Box 304, Houston, TX 77030, USA
e-mail: cioannid@mdanderson.org;
constantinioannides@gmail.com

Present Address:
C. L. Efferson
Merck Corporation, Boston, MA, USA

TLR-2. Experimental verification of our findings is needed to create synthetic adjuvant for vaccines. Such synthetic PGN can direct both adjuvant and cancer antigen to TLR-2.

Keywords PGN monomers · Charged peptides · Bind TLR-2 · Molecular simulation

Abbreviations

PGN	Peptidoglycan
TLR-2	Toll-like receptor 2
NOD-1/2	Nucleotide-binding oligomerization domains 1 and 2
PGRP	Peptidoglycan recognition proteins
ECD	Extracellular domain
DG	Free energy
LPS	Lipopolysaccharide
DAP	Meso-diaminopimelic acid
MDP	Muramyl-dipeptide or <i>N</i> -acetyl-muramyl-L-alanyl-D-isoglutamate
MTP	Muramyl tripeptide = MDP extended with lysine
NAG	<i>N</i> -acetyl-glucosamine
NAM	<i>N</i> -acetyl-muraminic acid
LRR	Leucine-rich repeat
iMDC	Immature monocyte-derived DC
HA	Haemagglutinin
PGN-ASK	[NAG-NAM-Ala-(L-Ser)-Lysine
ER	Endoplasmic reticulum
kcal	Kilocalories per mol
unbound TLR-2	TLR-2 modeled on TLR-3 ectodomain
bound TLR-2	TLR-2 modeled on lipopeptide-bound TLR-2:TLR-1 heterodimer

Introduction

The two most commonly studied components of Gram-positive and Gram-negative bacterial cell wall are PGN and LPS, respectively. The PGN concentration is far greater in the walls of Gram-positive bacteria than in Gram-negative bacteria.

PGN is constituted of glycan strands of two alternating sugar derivatives, NAG and NAM. NAG and NAM form the disaccharide subunit. The carboxyl group of NAM is linked to a stem peptide. The stem peptide consists of four or five alternating L- and D-amino acids. This structure is highly cross-linked by inter-peptide bridges. Most Gram-positive *cocci* such as *Staphylococcus aureus* have a stem peptide made of L-Ala-D-Gln-L-Lys-D-Ala-D-Ala. Bacilli and Gram-negative bacteria have a stem peptide with lysine replaced by L-meso-diaminopimelic (DAP). Lysine

of one PGN unit is linked via an inter-peptide bridge to the lysine of the next PGN unit. *S. aureus* PGN has a pentaglycine bridge [1]. The link continues until a polymeric PGN structure is formed [2]. PGN are recognized by 3 distinct innate immune receptors NOD1/2, PGPR, and TLR-2.

TLR1, ubiquitously expressed, is involved mainly in the recognition of Gram-negative bacteria. The PGN ligand of NOD1 contains NAG-NAM-L-Ala-D-Gln-DAP. NOD2, expressed in monocytes/macrophages detects PGN from Gram-negative and Gram-positive bacteria. NOD2 recognizes MDP, the minimum PGN, capable of biological activity, common to both classes of bacteria and MTP (MDP extended with lysine) [3]. PGPRs in mammals can process and bind enzymatically processed PGN.

PGN polymer is reduced in cells to monomer (PGN monomer) by autolysins (DD/DL), carboxypeptidases and endopeptidases, which cut the “inter-peptide bridge”. PGN is reduced to MTP by *N*-acetyl-glucosaminidase and to non-functional tri-peptide by *N*-acetyl-muramidase. The diversity of Lys-type PGN is limited. The free carboxyl group of D-glutamic acid of the stem peptide can be amidated (to glutamine) or linked to another amino acid, e.g., glycine or D-serine. Most PGN polymers are reduced in vivo by proteases to PGN tetramers, dimers, and monomers [4]. Asong et al. [4] reported that PGN fragments formed by remodeling of PGN by the autolysins bound TLR-2 with moderate to high affinity. The authors proposed that TLR-2 evolved to recognize a limited number of Lys-containing PGN motifs to avoid over-activation of immunity. PGN containing DAP was more potent than PGN containing Lys from *S. aureus*. The higher potency of DAP-PGN than of Lys-PGN may be due to its free carboxyl group, which binds TLR-2.

It was proposed that Lys-type PGN activates TLR-2 and NOD-2, whereas MDP and MTP activate NOD1 [1, 3]. Structural diversity of PGN makes difficult to identify specific responses and ligands. It is unknown which elements of TLR-2 are recognized by PGN. The involvement of TLR-2 in recognition of PGN and initiation of inflammation has been controversial. Highly purified PGN did not activate TLR-2 and production of IL-6 and TNF- α through TLR-2 but did activate the intracellular Nod1 [5]. A second study by Dziarsky and Gupta challenged the conclusions of the first study [6]. A third study showed that histamine enhances TLR-2 expression and IL-6 production [7], while a fourth study [8] proposed that PGN can quickly activate TLR-2 in monocytes/macrophages. This study used high/non-physiological amounts of PGN such as 30 μ g, described in the first study. PGN monomer is less activating than tetramer [9].

Lipids and lipopeptides activate monocytes and dendritic cells [10]. Lipopeptides activate TLR-2 and TLR-4

through their palmitoic acid chains, bound to a charged peptide ($\text{PAM}_3\text{-CSK}_4$). The fatty acid chains insert in each TLR monomer (TLR-2 and TLR-1/TLR-6), while the peptide, left outside, holds the monomers together [11–13]. TLR-2 activated by lipoteichoic acid (LTA) was found in endolysosomes and trafficked to Golgi and endoplasmic reticulum. This antigen presentation pathway delivers peptides to proteasome [14].

S. aureus PGN cannot cause shock, by itself but cooperate with LPS to induce TNF- α and IFN- γ and provoke septic shock. Aseptic peritonitis due to *S. aureus* has been reported; PGN monomer is apyrogenic compared with MTP [15, 16].

We hypothesized that synthetic PGN is significant to create specific and soluble adjuvant, free of LPS [4, 16, 17]. Since TLR-2 can deliver LTA to endoplasmic reticulum, it can also deliver peptides and short proteins too.

Knowing where the PGN, MDP, MTP, and peptides bind TLR-2 and some indications of their binding affinity is significant to specifically activate TLR-2 with physiological concentrations of PGN. Blocking peptides, which bind the same site with the stem peptide of PGN can be designed to inhibit activation of all TLRs. We addressed these questions, in silico, using novel methods in molecular modeling and quantification of binding affinity, as docking energy.

The literature shows that (a) PGN tetramer is a stronger activator than the PGN-dimer [9]; (b) the “inter-peptide bridge” is needed for activation of TLR-2 by PGN [6]; (c) PGN containing L-amino acids must be detected by receptors; (d) IL-6 produced by many cell types including dendritic cells, in response to PGN is an indicator of TLR-2 activation [5].

We found that mutated PGN with L-serine (Ser) replacing D-glutamine (Gln) docked to unbound TLR-2 modeled but not to bound TLR-2. The unbound and bound TLR-2 were modeled using the structures of unbound TLR-3 and lipopeptide ($\text{Pam-}\text{CSK}_4$)-bound TLR-2, respectively. PGN-ASK [NAG-NAM-Ala-(L-Ser)-Lys] binds TLR-2, 403–430 with high affinity and TLR-2, 227–237 with low affinity, but not the Pam-CSK4-binding site. Both L-Ser and L-Lys bound TLR-2, suggesting the entire PGN monomer, except the inter-peptide bridge, is needed for binding.

Charged peptides alone did not induce IL-6 but significantly increased or decreased the amount of IL-6 induced by physiological concentrations [5, 6] of 50–100 ng PGN. PGN did not induce IL-12 in iMDC when IFN- γ was not added to cultures. Our findings suggest a novel mode of TLR-2 di- or tetramerization by PGN. PGN inserts NAM-NAG in C-terminal ECD of TLR-2, and the pentaglycine bridge brings close 3–5 TLR-2 molecules. MDP and MTP preferentially bind the N-terminus of TLR-2.

Materials and methods

S. aureus PGN was obtained from Biochemika. MDP was from Calbiochem. Repurified, protein-free *E. coli* K235 LPS was obtained from Calbiochem and was used as prototypic TLR4 agonist. The natural TLR-2 agonist, tri-palmitoyl-S-glycyl-cysteine (Pam_3Cys), was obtained from Sigma. FITC-conjugated antibodies to TLR-2 (TL2.1, TL2.3), TLR-3, TLR-4, CD13, CD14, CD1a, and CD3 (for MDC) were obtained from BD Pharmingen.

Peptides

Peptides B69R, *LVSEFSRMARDPQ*, and C43, *RFRELVSEFSRMAR*, correspond to HER-2 (972–986) and HER-2 (968–982), respectively. Influenza hemagglutinin peptides are as follows: M128, 341–350, *GLFGAIAGFL*, and M119,HA, 98–110, *GDFIDYEEELREQL*. M128 is a control peptide that lacks charged residues. M119 is an anionic (acidic) peptide. M119 is part of the charged HA-head. TLR-2 peptides are M120 (312–328) [*TIR-RLHIPRFYLFY*] cationic and M124 [*LTIDDLIPDFYLF*] anionic. M124 is a control for charged residues in M120. The cations in M120 were replaced, in M124, with anions. M120 is expected to bind to anions (below). Peptides were synthesized and purified by MDACC Synthetic Antigen laboratory.

Homologous modeling

To generate unbound TLR-2, we loaded the sequence of ECD of TLR-2 (NCBI Reference Sequence: NP_003255.2, amino acids 1–586) to Swiss-Pdbviewer (<http://spdbv.vital-it.ch>). We used as a template the TLR-3 ectodomain [18]. After alignment and fit of the homologous domains, the model was submitted to Swiss-Model server (<http://spdbv.vital-it.ch>). The most stable tri-dimensional structural model and its minimal energy were determined with the Swiss-pdb Viewer. Comparison of sequences and alignments was made by FASTA as described [18, 19]. As docking control, bound TLR-2, we used the TLR-2 structure extracted from the crystal structure of TRL-2-TLR-1 bound by lipopeptide [12].

The structures of PGN were reported [20, 21]. We replaced, D-Gln with L-Ser. We reconstituted the 3D structures of MDP, of lysine-type MTP, and of PGN-S-monomer. We omitted the “bridge” to be closer to conditions when PGN is processed by carboxy- and endopeptidases.

PGN is contained in the PDB file of 2EAX [21]. We constructed PGN-S-dimers by linking 2 PGN-M-S molecules with 5 consecutive glycines. The C-terminal Gly of the first bridge linked to the Lys of the second PGN-M-S

(Fig. 1a). PGN-T was formed by linking 2 PGN-M-S dimers through NAG (not shown).

Identification of the PGN-M-S and peptide-binding sites in ECD-TLR-2 by molecular docking

We used the program Autodock4 (<http://autodock.scripps.edu>). The ligand was inputted as a macromolecule with charged residues. The TLR-2 amino acids were designated as flexible residues. Each sequence of ECD tested by the Auto-Dock was designated as *docking box*.

The affinity of ligand for the sites on ECD-TLR-2 is shown as negative (= released) free energy (−DG) in kcal. DG = −[0.1–1.0] kcal was considered weak binding. The +DG indicates that the ligand binds target when the external energy is higher than the number of calories listed. PGN and peptides docking with +DG < 0.050 kcal or 50 cal were considered potential binders (*at equilibrium with receptor*). The equilibrium changes toward binding when heat increases, even little, above 37°C. Heat also

induces conformational changes in PGN [22]. High positive (+) DG of >500 cal/0.5 kcal indicates PGN will not bind TRL-2.

Graphic presentation was made with PyMol [<http://pymol.sourceforge.net/><http://www.pymol.org>].

Activation of immature, monocyte-derived DC (iMDC) by PGN

Monocytes were isolated from PBMC of healthy donors and cultured in GM-CSF plus IL-4 as we described [23–25]. They expressed CD14 and lacked CD13. Expression of TLR-2 was confirmed by staining with TLR-2.1 mAb. iMDC were stimulated with 50 or 100 ng of PGN in serum-free medium. Similarly, iMDC in serum-free medium were pulsed with peptides at indicated concentrations for 1.5 h before PGN was added. IFN- γ was added for fast induction of IL-12. Supernatants were collected 16 h later. IL-6 and IL-12 were quantified with ELISA (R & D Systems).

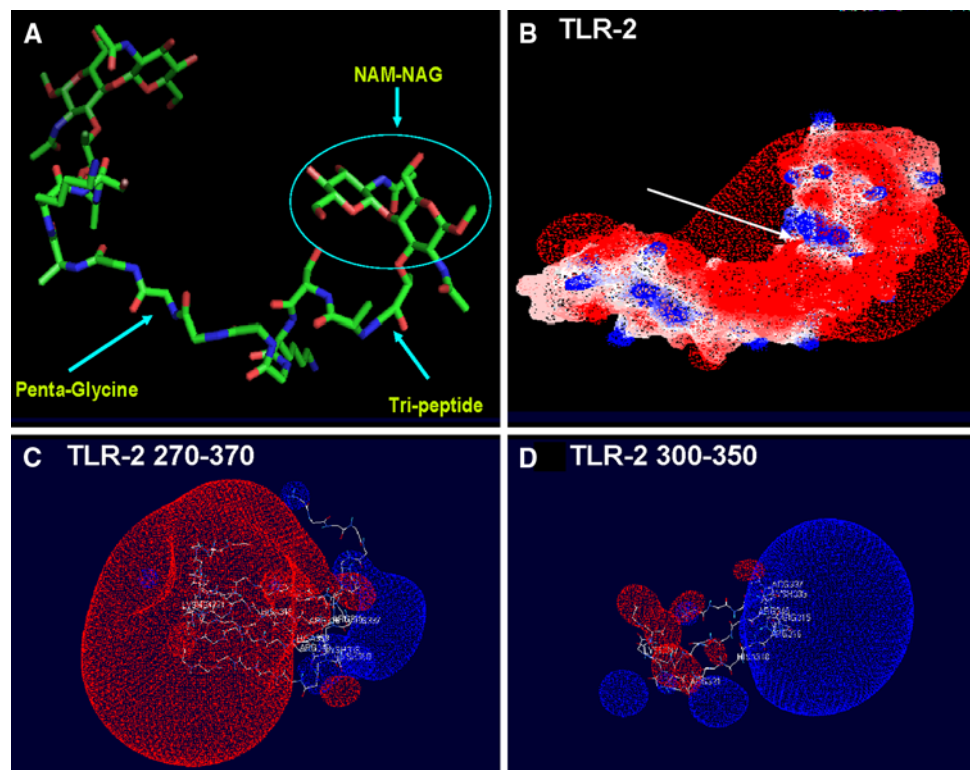


Fig. 1 Models of PGN and of ligand-binding sites on TLR-2. **a** PGN-dimer. NAG-NAM, stem peptide (Ala-[L-Ser-]-Lys) linked by pentaglycine to the second PGN. NAM-NAG, stem tripeptide and pentaglycine are shown with arrows. The figure was made with the program PyMOL. See “Materials and methods” for details. **b** Map of the electrostatic potential of the ECD-TLR-2. Anionic areas are shown in red here and in the following figures. The cationic areas are

shown in blue in this and in the following figures. The figure was made with software SwissProtein. See “Materials and methods” for details. **c** The Pam₍₃₎-CSK₍₄₎ binding site and its surroundings on ECD-TLR-2, 270–370. The area consist of a large anionic (the larger the circle the higher the charge) followed by a weak (small) cationic area. **d** Enlarged weak cationic area TLR-2, 300–350. Figure made with the graphics program SwissProtein

Results

Positively and negatively charged areas in TLRs

We constructed models of the “unbound” ECD-TLR-2. Cationic and anionic amino acids alternate in LRRs (Fig. 1b, c, d; S-Figure 1A, B, shown in red and blue, respectively). Published results show that the TLR2:TLR1 hetero-dimer is activated by the 3 palmitoic acid chains linked to cysteines of Pam₍₃₎-CSK₍₄₎ and N-Pam-S-Lauryl-CSK₍₄₎. Lysines play a minor, stabilizing role, filling the channel TLR-1:TLR-2. The amino acids in the sequence TLR-2, 305–333 form the interface TLR-1/TLR-2 and bind the lipid [12, 13] (Fig. 1c, d). However, the PGN-S-monomer does not bind TLR-2, 312–324 (DG = 0.67 kcal). Therefore, binding of PGN to or close to lipopeptide-binding site is unlikely. We then searched for positions in TLR-2 where PGN can bind with higher affinity.

We hypothesized the cations and anions in TLR-2 bind anionic and cationic peptides, respectively. To identify peptide acceptor sites, we searched in ECD, for sequences, which contain at least four amino acids of the same charge, over ten consecutive amino acids. We found such sequences in TLR-2, 252–262, TLR-2, 281–286, and TLR-2, 313–324 (Fig. 1d). Four phenol rings (R-FYLFY-D), in the middle of the sequence, will interact with lipids and form H-bonds [12, 13].

To detect positions of peptide binding, we used as probes peptides M124 and M120. M124 has replaced all cations of M120 with anions. Peptide M120, TLR-2 (315–324) is more charged than the peptide TLR-2, 252–261. M120 has three double(R) and one single (H) cation and one anion (E), whereas TLR-2, 252–261 has one double plus four single cations.

Charged peptides modulated the amount of IL-6 induced by PGN

To address whether peptides affect cytokine induction by PGN, we quantified IL-6 and IL-12 produced by GM-CSF + IL-4 cultured iMDC. IL-6 produced by endothelial and epithelial cells transfected with TLR-2 is a general indicator of TLR-2 activation [5]. Production of IL-12 is restricted to monocytes/macrophages and dendritic cells and indicates these cells’ pro-inflammatory conditioning.

M120, M124 and all other peptides used did not induce IL-6. PGN alone at 50 ng/ml and 100 ng/ml induced IL-6 and not IL-12 in iMDC. This finding also suggests that our PGN was not contaminated with LPS.

M120 augmented the amount of IL-6 induced by 50 ng PGN by almost threefold (Fig. 2a). Compared with 50 ng PGN alone, PGN + M120 increased IL-6 by almost threefold. The amount of IL-6 induced by 250 ng of PGN

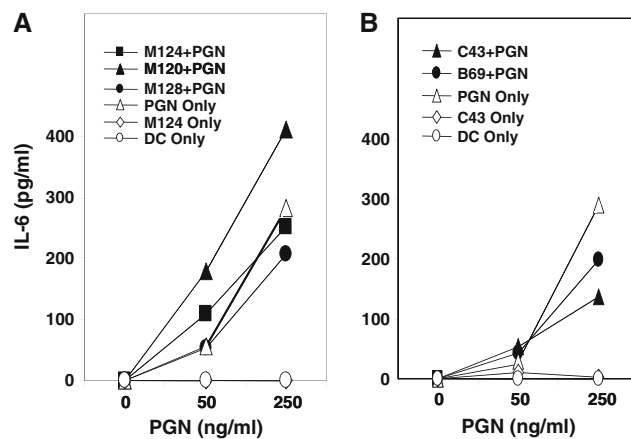


Fig. 2 Modulation of IL-6 induction by PGN by the cationic and aromatic peptides M120 and C43. **a** M120 increased IL-6 production by iMDC activated by PGN. M124 and negative control peptide M128 had no effect. Results of duplicate determinations with differences between replicates <10%. **b** C43 inhibited production of IL-6 by iMDC activated by PGN by 65%. Results of duplicate determinations with differences between replicates <10%. B69 did not significantly inhibit IL-6 production, compared with PGN alone (35% inhibition)

increased to 380 pg/ml, thus the synergistic effect of M120 was smaller with 250 ng/ml PGN than with 50 ng PGN/ml.

In contrast, M124 pre-incubated with 50 ng/PNG had a weak effect. M124 had no effect when pre-incubated with 250 ng PGN, suggesting that induction of IL-6 by PGN-alone induction reached its maximum.

To confirm that the effects were due to bound peptides, we repeated the study, with the same iMDC using C43 and B69. C43 has cations at both N- and C-termini and anions in the middle. B69 lacks the first 4 cations of C43 at N-terminus. B69 is extended with 3 amino acids at its C-terminus compared with C43. Its cations are in the middle of the peptide and are flanked by anions.

C43 inhibited IL-6 induced by 250 ng/ml PGN, by 60%. B69 inhibited IL-6 induced by PGN by only 34% (Fig. 2b). Therefore, charged peptides, C43 and M120, synergized or antagonized IL-6 induction by PGN. M120 and M124 increased the amount of IL-12 induced by PGN in the presence of IFN- γ by 40–60%. This increase was not considered significant (S-Table I).

Charged peptides bind to TLR-2 (434–455)

M120 is part of TLR-2 interface interacting with TLR-1. Thus, M120 cannot react with TLR-2 in this position. We mapped the DG of binding energy of M120 and M124 over the entire sequence of ECD. M120 [TI-R³ - R⁴ - L-H⁶ IP-R⁹ - FYLFY] and M124 bound TLR-2, 434–454, with high affinity (DG = −24.00 and −36.00 kcal, respectively). C43 bound the same site with 20 times lower affinity than

M120 ($\Delta G = -1.00$ kcal). Control, M128, was at equilibrium with TLR-2, 434–455 and did not bind to any site of TLR-2 bound by the other peptides. Similarly, B69R did not bind TLR-2, 227–237, 234–238, and 434–454 but is at equilibrium with TLR-2, 87–113.

M128 and B69 will bind these sites if the heat increases (Table 1).

TLR2, 434–455 of sequence WPEKMKYL-NLSSTRIHSVTGCI has a cationic “grid” [Lys⁴³⁷, Lys⁴³⁹, Arg⁴⁴⁷ and His⁴⁴⁹], which is surrounded by anions and polar amino acids, Glu⁴³⁶, Glu⁴⁶⁰, and Met⁴²⁸ (Fig. 3a, b).

Binding of M120 suggests that the side chains of Arg³ are attracted by Glu⁴⁶⁰ and Glu⁴⁸¹, and of Arg⁴ by Glu⁴⁸¹. Glu⁴³⁰ attracts His⁶ while Thr⁴⁰⁸, Met⁴²⁸ and Glu⁴³⁰ attract Arg⁹. Only 9 amino acids enter this pocket. Aromatic amino acids (FYLFY) did not insert in TLR-2. Fig. 3a (grey area). Cations interact with amino acids in several LRR-repeats in ECD [from Thr⁴⁰⁸ to Glu⁴⁸¹] (Fig. 3a; S-Figure 2A).

C43, R¹-F²-R³-E⁴-LVSEFSRMAR, inserts 8–9 N-terminal amino acids in TLR-2 coil, leaving FSRMAR outside. Arg¹ interacts with Met⁴²⁸; Phe² with Ser⁴⁵⁰ and Glu⁴³⁶; Arg³ with Tyr⁴⁸³, while is repulsed by Arg⁴³⁶. Asp⁴ forms H-bonds with Cys⁴⁵⁴ and Pro⁴⁵⁶. The binding affinity of C43 to TLR-2 is 10 times lower than of M120, probably because C43 has less cations than M120 and forms less electrostatic bonds with the TLR-2 (S-Figure 2A).

The significance of the N-terminal cation, for peptide binding, to TLR-2, 434–455, is confirmed by lack of binding of B69R. B69R maintains only the sequence LVSEFSRMAR of C43. Its first basic amino acid is Arg⁷.

M124 [LTIDDDIPDFY¹²-L¹³-FY¹⁵] binds by a different mechanism. It inserts its Tyr¹² and Tyr¹⁵. Tyr¹⁵ contacts Pro⁴³⁵ and Glu⁴³⁶. Tyr¹² contacts Glu⁴³⁶ and Pro⁴³⁵. Leu¹³ interacts with Leu⁴¹⁰, Thr⁴¹¹ and Leu⁴¹². Anions 1–10 are outside the pocket (Fig. 3b, dark grey; S-Figure 2B). M120 and M124 contain the same aromatic

amino acids at C-terminus. The need for cations for binding through peptide N-terminus is confirmed by lack of binding of control anionic peptide, M119 to TLR-2, 434–455.

C-terminal tyrosine of anionic M124 bind with higher affinity to TLR-2, 434–455 than cationic peptides.

PGN binds TLR-2 (403–430)

PGN-M has 2 sugars, NAG and NAM, linked to each other. Fig. 4a shows that NAG (red hexagon) is positioned between a large red field, Glu⁴³⁰ followed by Pro⁴²⁹, and a small blue field. NAM (small pentagon) is close to the large blue field, which covers the right side of the figure Ser⁴²⁷, Leu⁴⁰², and Glu⁴⁰³. The terminal lysine contacts Glu⁴⁰³ and Tyr³⁷⁸. Thus, PGN inserts its glycan head at C-end of the pocket and anchors to Glu⁴⁰³ and Tyr³⁷⁸ at the N-end of the pocket.

PGN-S-monomer binds with high affinity to TLR-2, 403–430 ($-\Delta G \leq 100$ kcal), and with low affinity to TLR-2, 227–233 ($-\Delta G = 0.005$ kcal). PGN-S-monomer is at binding equilibrium with TLR-2, 257–262 and TLR-2, 272–286 ($\Delta G = 0.008$ and 0.004 kcal, respectively) (Fig. 4b, c).

PGN-S-monomer did not bind TLR-2, 87–113 ($\Delta G = 12$ kcal) and TLR-2, 118–138 confirming its specificity for TLR-2, 403–430/417–428 (S-Figure 3B, Table 1).

The MTP (NAM-Ala-Ser-Lys) did not bind TLR-2, 404–430 and 434–455 (M-ASK, Fig. 3a; Table 1). MTP weakly bound TLR-2, 93–138 with $\Delta G > -1.00$ kcal. MDP/NAM-Ala-Ser, lacks the C-terminal Lys of MTP and is at binding equilibrium with TLR-2, 87–113 ($\Delta G = 0.065$ kcal) (S-Figure 3C, M-AS) NAG-NAM-Ala-Ser bound to TLR-2, 87–113 with low affinity, ($\Delta G = -1.85$ kcal) (S-Figure 3D, NM-AS). However, NAG-NAM-Ala-Ser did not bind TLR-2, 417–428 ($\Delta G = 1.50$ kcal) (not shown). Therefore, PGN-S-monomer needs NAG and L-Lys to bind with high affinity to TLR2, 404–430 or 417–428.

Docking of PGN was repeated with the “bound TLR-2” (Fig. 4d). PGN is at equilibrium with the C-terminus of the bound TLR-2: 572–586 ($\Delta G = 0.0026$ kcal). DG of binding of PGN on other ECD-TLR-2 positions was: TLR-2, 87–117 > 1,000 kcal, TLR-2, 200–240 > 600 kcal, TLR-2, 330–360 > 900 kcal; TLR-2, 435–470 > 400 kcal; TLR-2, 470–500 > 1,620 kcal; TLR-2, 500–540 > 1,300 kcal and TLR-2, 540–575 > 72 kcal. If temperature increase PGN can bind TLR-2, 572–586 while MTP can bind TLR-2, 227–238 (Table 1).

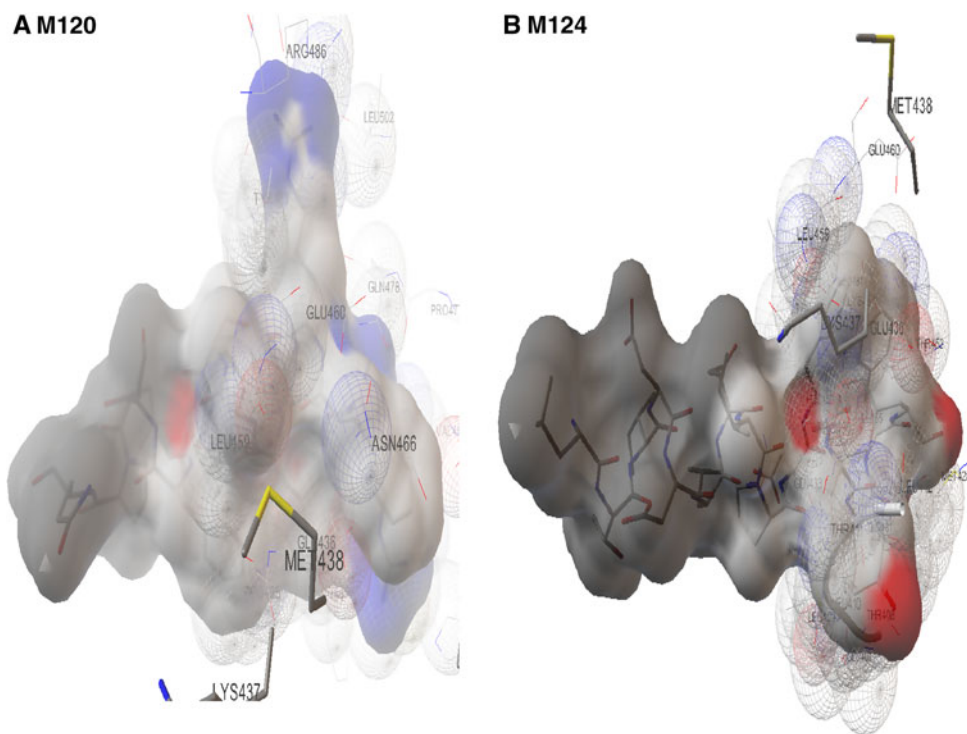
The complex of TLR-2-TLR-1 interacting with an agonist was obtained after the last 85 amino acids of TLR-2 were replaced with those of the hagfish VLRB.61 [12]. The

Table 1 TLR-2 sites bound by short peptides with highest affinity

Ligand	Target TLR-2, ΔG (kcal/mol)			Target MTP, ΔG (kcal/mol)
	87–135	234–238	434–455	
PGN-M-S	477	-0.005	2.150	N/A
MTP	-1.00	2.20	1.270	N/A
M120	7.480	257	-24	-3.91
M124	2.790	0.020	-36	-0.91
M119	418	374	143	2.60
M128	613	5.030	0.002	1.93
C43	5.320	123	-1.00	-0.01
B69R	0.071	60.1	22	0.18

The DG was quantified with the Auto-Dock 4 program. A low-affinity site of PGN-M-S is on TLR-2, 234–238

Fig. 3 Models of binding of the peptides M120 and M124 to TLR-2 (434–454). **a M120.** **b M124.** Complexes of peptides docked to TLR-2. The figure was extracted from AutoDock-4 and was made using the program PyMol. Peptides are shown as sticks in the ball structure of TLR-2. Details are shown in S-Figure 2. **a** Peptide outside TLR-2 is in light grey and **b** dark grey



sequence of crystallized TLR-2 ends at amino acid 500. In addition, the trimolecular complex, TLR-1-hagfish-TLR-2-hagfish-Pam₍₃₎-CSK₍₄₎, was inseparable at gel filtration. The high stability of the complex was recently reported to be due to a complex network of H-bonds. The H-bonds complex does not permit binding of other molecules to the trimer [26, 27]. Therefore, only a narrow region, TLR-2, 324–500, or TLR-2, 377–500, is left for PGN and peptide to bind “bound TLR-2”. We do not know whether this region is accessible to PGN. Our results show that PGN and peptide do not bind the charged residues in this region. Future studies will test whether binding occurs through H-bonds.

Binding of peptides to PGN and MTP

M120 and M124 bind with low affinity to MTP (Table 1). None of the peptides analyzed bound to PGN-S-monomer. M124 is at equilibrium with PGN-S-dimer ($DG = 0.030$ kcal). In conclusion, peptides tested have higher affinity for TLR-2 than for PGN and MTP.

Discussion

Peptides containing basic amino acids at their N-terminus and/or tyrosine at their C-terminus bind TLR-2 and modify cytokines produced by iMDC in response to PGN. To

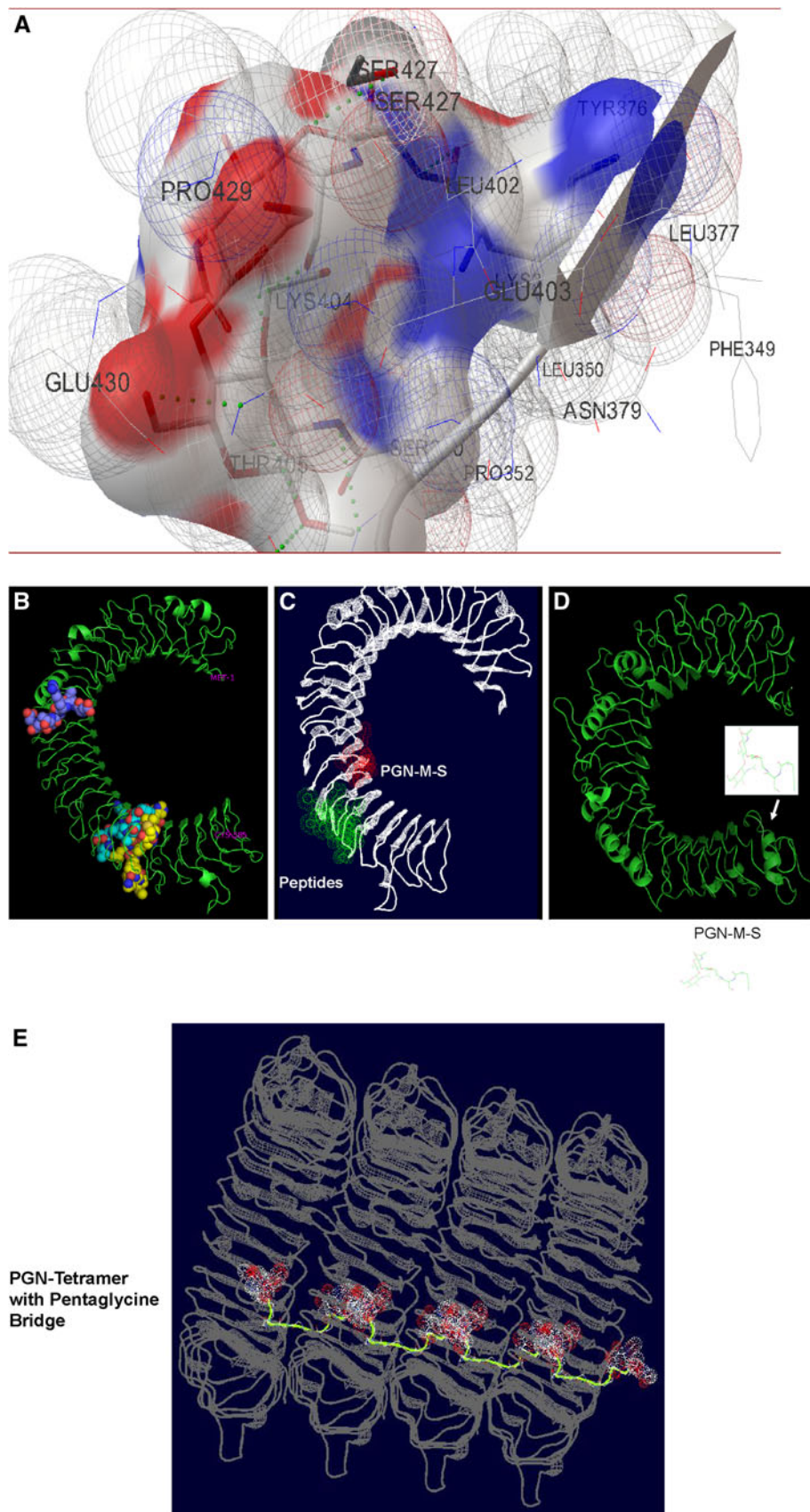
identify the binding sites of peptides and PGN, we mapped their docking to at least 30 consecutive sites encompassing the entire ECD-TLR2. We identified a binding site, TLR-2, 434–455, for peptides M120, M124, and C43. Each peptide appears to interact with at least 2 LRRs and not with a linear stretch of amino acids.

We also identified a high affinity binding site, TLR-2, 403–430, for PGN-S-monomer. In additional dockings, we identified TLR-2, 417–428 as the site with minimum length bound by PGN-S-monomer (not shown). This site precedes with 6–7 amino acids the high-affinity binding site of peptides. A low-affinity site for PGN-S-monomer is TLR-2, 227–233. The continuous PGN and peptide-binding pocket appear unique in its organization. These findings are novel and have not been reported before.

The high-affinity binding sites of peptides and PGN are close to each other. PGN and peptides enter through different doors. PGN-S-monomer enters through TLR-2 internal (convex) face, while peptides through external face of TLR-2. “Inside”, PGN-S-monomer and peptides can interact. M120 binds within the designated pocket of PGN-S-monomer (i.e., Arg¹⁰ with Thr⁴⁰⁸, Met⁴²⁸, and Glu⁴³⁰). C43 also binds Met⁴²⁸, designated as link for PGN-S-monomer (Arg¹ with Met⁴²⁸).

Met⁴²⁸ is a critical residue for activation by PGN, because if it is blocked by C43, activation of TLR-2 decrease. Leu⁴¹⁰, Thr⁴¹¹, and Leu⁴¹² form van der Waals forces, too weak to affect activation of TLR-2.

Fig. 4 a The PGN-S-monomer binds with high affinity to TLR-2, 403–430. PGN-S-monomer inserts NAG (large red hexagon) and forms H-bonds with Glu⁴³⁰. H-bonds are shown with dots. NAM is shown as a small red pentagon. It forms H-bonds with Ser⁴²⁷ and Lys⁴⁰⁴. Lysine of the stem peptide contacts Glu⁴⁰³ and Tyr³⁷⁶. PGN is sandwiched between a large red and a large blue field. **b** Peptides bind TLR-2 (434–454) opposite to PGN-binding site. PGN (in blue) bound the low affinity sites TLR-2, 227–237 and 87–113. The peptide is in yellow in both figures. Peptides (balls) and TLR-2 (string) model. **c** Same model as in B. Peptide (Green), PGN (Red), TLR-2 (White). **d** PGN can bind the C-terminus of the lipopeptide-bound TLR-2. The TLR-2 structure was obtained from the crystal structure TLR-2: Pam-CSK:TLR-1.(Reference 11). PGN binding was repeated at least 4 times, using 4 different docking amino acids. A small increase in external energy (temperature) will suffice PGN to bind TLR-2. **e** Proposed model of activation of multiple TLRs by PGN tetramer. PGN is inserted in NAM-NAG and each “unbound” TLR (TLR-2, TLR-1, TLR-6). Three pentaglycine bridges linking Lys can bring 4 TLRs closer. At higher temperature, PGNs can cooperate with Pam-CSK bringing close 4 TLR-2 molecules. Lipopeptides bind and activate groups of 2 TLRs



Cooperation PGN lipopeptide in natural TLR-2 activation?

We propose a novel model of TLR-2 activation by PGN. NAG, NAM, Ala, and L-Ser fill the TLR-2 pocket, while Lys protrudes from the pocket. Lys is linked to the peptide bridge (Fig. 4a). One bridge can bring two TLR-2 molecules closer, while three bridges can bring together four TLR-2 molecules. The PGN tetramer has 3 bridges (Fig. 4e). Amino acids TLR-2, 417–428 are on the internal face of TLR-2. Our hypothesis engenders support from the findings that PGN tetramer is the strongest activator of TLR-2 and two binding models derived from analysis of PGN monomer bound to PGRP-I β [9, 21, 26].

In the first, the stem peptide is held in extended conformation at the deep end of the binding groove; NAG-NAM fills a pocket in the middle of this groove [21]. The second model proposed how PGRP interacts with bacterial cell wall. PGN strands form a honeycomb. Strand's cross-linking determines the size of honeycomb pores. Complete cross-linking of PGN monomer reduce, while incomplete cross-linking enlarge each pore [28]. TLR-2 inserts its ECD in the hexagonal or octagonal PGN honeycomb-shaped pores. A large fragment of bacterial cell wall has more pores; thus, more TLR2, TLR-1 and TLR6 molecules are brought together. We do not know how deep ECD inserts in the pore. Our simulation of binding did not confirm the site TLR-2, 40–64 but confirmed that a binding site for natural PGN in exist in TLR-2, 30–305 [29].

Lipopeptides bind TLR-2, 274–333. This long TLR-2 site contains sub-sites with different charges: TLR-2 (281–286, ELEFDD) has 4 acidic residues. M120 did not bind to this site. Other 12- to 14-amino acid-long charged peptides bound this site with low affinity ($-DG \leq 0.010$ kcal). The next LRR coil, 317–323, HIP-RFYL contains basic and aromatic amino acids. It has the same sequence with M120, thus M120 cannot bind. M124 also does not bind. This site forms the interface of TLR-2–TLR-1 [12, 13]. None of the peptides tested by us bound to this site. Thus, Pam-CSK can bind this site.

PGN bring close 4 TLR-2 molecules. Pam-CSK binds to 2 TLR molecules and activate 2 groups of 2 TLRs. Alternatively, the free NAM-NAG of PGN honeycombs surround and dock TRLs and lipopeptides activate groups of 2 TLRs.

Our findings support the hypothesis that PGN binds and activate TLR-2 [6]. Digestion of PGN with muramidase that hydrolyzes glycosidic bonds between NAM and NAG decreased the TLR2-2-dependent activation by PGN [6]. Our results also confirm the significance of NAG and of the stem peptide in TLR-2 activation.

TLR-2 is internalized upon interaction with ligand, specific antibody or “pseudo-ligand” in adjacent cells.

TLR-2 internalization by its specific antibody resulted in the presentation of a peptide from that antibody to peptide specific CD4 $^{+}$ cells [29]. TLR-2 can carry short antigens, which activate T cells [30]. TLR-2 activated by lipoteichoic acid (LTA) was found in endolysosomes and trafficked to Golgi and endoplasmic reticulum. Immunization with glycans composed of a covalently linked TLR-2 synthetic agonist, T cell helper peptide and a tumor-associated glycopeptide induced more IgG specific for the glycopeptide than lipid adjuvant [31].

We hypothesize that we can pulse APC with PGN plus a peptide tumor antigen extended with R-rich (N-Terminus) or Tyr-rich (C-terminus) anchors. Binding of PGN-S-dimer/tetramer may internalize TLR-2 and release the tumor antigen peptide in endoplasmic reticulum. This approach may be useful to present more molecules of tumor antigen by the APC, which have low levels of MHC-I. PGN ligands can activate APC and increase MHC-I expression on APC. The efficiency and significance of Ag-presentation to CD8 $^{+}$ cells through TLR-2 will be elucidated in future studies.

To conclude, we identified by molecular simulation that PGN monomer composed of L-amino acids can bind with high affinity to a specific site in TLR-2. The site is located at a distinct position than the binding site of Pam-CSK site. We identified a docking site for MDP/MTP, which is distant from the PGN site. We also found that R-rich and Tyr-rich peptides bind TLR-2 close to the PGN site and increase significantly IL-6 production in response to low, nanogram level (“physiological”) amounts of PGN above the levels induced by PGN-alone in serum-free media.

Acknowledgments This research was supported by License funds for Discretionary research from Apthera Corporation.

References

1. Fournier B, Philpott DJ (2005) Recognition of *Staphylococcus aureus* by the innate immune system. Clin Microbiol Rev 18(3):521–540
2. Meroueh SO, Bencze KZ, Hesek D, Lee M, Fisher JF, Stemmler TL, Mobashery S (2006) Three-dimensional structure of the bacterial cell wall peptidoglycan. Proc Natl Acad Sci USA 103:4404–4409
3. Kim Y-G, Park JH, Shaw MH, Franchi L, Inohara N, Gabriel Nunez G (2008) The cytosolic sensors Nod1 and Nod2 are critical for bacterial recognition and host defense after exposure to toll-like receptor ligands. Immunity 28:246–257
4. Asong J, Wolfert MA, Maiti KK, Miller D, Boons GJ (2009) Binding and cellular activation studies reveal that toll-like receptor 2 can differentially recognize peptidoglycan from gram-positive and gram-negative bacteria. J Biol Chem 284(13):8643–8653
5. Travassos LH, Girardin SE, Philpott DJ, Blanot D, Nahori MA, Werts C, Boneca IG (2004) Toll-like receptor 2-dependent

- bacterial sensing does not occur via peptidoglycan recognition. *EMBO Rep* 5:1000–1006
6. Dziarski R, Gupta D (2005) *Staphylococcus aureus* peptidoglycan is a toll-like receptor 2 activator: a re-evaluation. *Infect Immun* 73:5212–5216
 7. Talreja J, Kabir MH, Fillia MB, Stechschulte DJ, Dileepan KN (2004) Histamine induces toll-like receptor 2 and 4 expression in endothelial cells and enhances sensitivity to gram-positive and gram-negative bacterial cell wall components. *Immunology* 113:224–233
 8. Aki D, Minoda Y, Yoshida H, Watanabe S, Yoshida R, Takaesu G, Chinan T, Inaba T, Hikida M, Kurosoaki T, Saeki K, Yoshimura A (2008) Peptidoglycan and lipopolysaccharide activate PLC-g2, leading to enhanced cytokine production in macrophages and dendritic cells. *Genes Cells* 13:199–208
 9. Filipe SR, Tomasz A, Ligoxygakis P (2005) Requirements of peptidoglycan structure that allow detection by the *Drosophila* toll pathway. *EMBO reports* 6(4):327–333
 10. Natsuka M, Uehara A, Yang S, Echigo S, Takada H (2008) A polymer-type water-soluble peptido-glycan exhibited both toll-like receptor 2 and NOD2-agonistic activities, resulting in synergistic activation of human monocytic cells. *Innate Immun* 14(5):298–308
 11. Meng G, Grabiec A, Vallon M, Ebe B, Hampel A, Bessler W, Wagner H, Kirschning CJ (2003) Cellular recognition of tri-/di-palmitoylated peptides is independent from a domain encompassing the *N*-terminal seven leucine-rich repeat (LRR)/LRR-like motifs of TLR2. *J Biol Chem* 278(41):39822–39829
 12. Jin MS, Kim SE, Heo JY, Lee ME, Kim HM, Paik SG, Lee H, Lee JO (2007) Crystal structure of the TLR1-TLR2 heterodimer induced by binding of a tri-acylated lipopeptide. *Cell* 130(6):1071–1082
 13. Jin MS, Oh Lee J-O (2008) Structures of the toll-like receptor family and its ligand complexes. *Immunity* 15:182–191
 14. Nilsen NJ, Deininger S, Nonstad U, Skjeldal F, Husebye H, Rodionov D, Von Aulock S, Hartung T, Lien E, Bakke O, Espelvik T (2008) Cellular trafficking of lipoteichoic acid and toll-like receptor 2 in relation to signaling: role of CD14 and CD36. *J Leukoc Biol* 84(1):280–291
 15. Martis L, Patel M, Giertych J, Mongoven J, Taminne M, Perrier MA et al (2005) Aseptic peritonitis due to peptidoglycan contamination of pharmacopoeia standard dialysis solution. *Lancet* 365:588–594
 16. Buskas T, Thompson P, Boons GJ (2009) Immunotherapy for cancer: synthetic carbohydrate-based vaccines. *Chem Commun (Camb)* 36:5335–5349
 17. Wolfert MA, Roychowdhury A, Boons GJ (2007) Modification of the structure of peptidoglycan is a strategy to avoid detection by nucleotide-binding oligomerization domain protein-1. *Infect Immun* 75(2):706–713
 18. Choe J, Kelker MS, Wilson IA (2005) Crystal structure of human Toll-like receptor 3 (TLR3) ectodomain. *Science* 309(5734):581–585
 19. Kubarenko A, Frank M, Weber AN (2007) Structure-function relationships of toll-like receptor domains through homology modelling and molecular dynamics. *Biochem Soc Trans* 35(6):1515–1518
 20. Guan R, Brown PH, Swaminathan CP, Roychowdhury A, Boons GJ, Mariuzza RA (2006) Crystal structure of human peptidoglycan recognition protein Ia bound to a muramyl pentapeptide from gram-positive bacteria. *Protein Sci* 15(5):1199–1206
 21. Cho S, Wang Q, Swaminathan CP, Hesek D, Lee M, Boons G-J, Mobashery S, Mariuzza RA (2007) Structural insights into the bactericidal mechanism of human peptidoglycan recognition proteins. *Proc Natl Acad Sci USA* 104:8761–8766
 22. Zhang M (2010) Heating-induced conformational change of a novel beta-(1→3)-D-glucan from *Pleurotus geestanus*. *Biopolymers* 93(2):121–131
 23. Efferson CL, Schickli J, Ko BK, Kawano K, Mouzi S, Palese P, García-Sastre A, Ioannides CG (2003) Activation of tumor antigen-specific cytotoxic T lymphocytes (CTLs) by human dendritic cells infected with an attenuated influenza A virus expressing a CTL epitope derived from the HER-2/neu proto-oncogene. *J Virol* 77(13):7411–7424
 24. Efferson CL, Tsuda N, Kawano K, Nistal-Villán E, Sellappan S, Yu D, Murray JL, García-Sastre A, Ioannides CG (2006) Prostate tumor cells infected with a recombinant influenza virus expressing a truncated NS1 protein activate cytolytic CD8+ cells to recognize noninfected tumor cells. *J Virol* 80(1):383–394
 25. Tsuda N, Chang DZ, Mine T, Efferson C, García-Sastre A, Wang X, Ferrone S, Ioannides CG (2007) Taxol increases the amount and T cell activating ability of self-immune stimulatory multimolecular complexes found in ovarian cancer cells. *Cancer Res* 67(17):8378–8387
 26. Kajava AV, Vasselon T (2010) A network of hydrogen bonds on the surface of TLR2 controls ligand positioning and cell signaling. *J Biol Chem* 285(9):6227–6234
 27. Drage MG, Tsai H-C, Pecora ND, Cheng T-Y, Arida RR, Shukla S, Rojas RE, Seshadri C, Moody DB, Boom WH, Sacchettini JC, Harding VC (2010) *Mycobacterium tuberculosis* lipoprotein LprG (*Rv1411c*) binds triacylated glycolipid agonists of Toll-like receptor 2. *Nat Cell Mol Biol* 17:1088–1095
 28. Guan R, Roychowdhury A, Ember B, Kumar S, Boons GJ, Mariuzza RA (2004) Structural basis for peptidoglycan binding by peptidoglycan recognition proteins. *Proc Natl Acad Sci USA* 101(49):17168–17173
 29. Mitsuzawa H, Wada I, Sano H, Iwaki D, Murakami S, Himi T, Matsushima N, Kuroki Y (2001) Extracellular toll-Like receptor 2 region containing Ser⁴⁰-Ile⁶⁴ but not Cys³⁰-Ser³⁹ is critical for the recognition of *S. aureus* peptidoglycan. *J Biol Chem* 276(44):41350–41356
 30. Schjetne KW, Thompson KM, Nilsen N, Flo TH, Fleckenstein B, Iversen JG, Espelvik T, Bogen B (2003) Cutting edge: link between innate and adaptive immunity: toll-like receptor 2 internalizes antigen for presentation to CD4+ T cells and could be an efficient vaccine target. *J Immunol* 171(1):32–36
 31. Ingale S, Wolfert MA, Buskas T, Boons GJ (2009) Increasing the antigenicity of synthetic tumor-associated carbohydrate antigens by targeting toll-like receptors. *Chembiochem* 10(3):455–463